Available online at www.sciencedirect.com

SCIENCE DIRECT®

Thin Solid Films 498 (2006) 289 – 293

thin solid films

www.elsevier.com/locate/tsf

Characterization and thermal stability of fluorosilicate glass films deposited by high density plasma chemical vapor deposition with different bias power

Wen-Chu Hsiao [a], Chuan-Pu Liu [a], Ying Lang Wang [b,*], Yi-Lung Cheng [c]

[a] Department of Material Science and Engineering, National Cheng Kung University, Tainan, Taiwan
[b] College of Science and Engineering, National University of Tainan, Taiwan
[c] Institute of Materials Science and Engineering, National Chiao-Tung University, Hsinchu 300, Taiwan

Available online 16 August 2005

Abstract

High-density plasma chemical vapor deposition (HDP-CVD) fluorosilicate glass (FSG) films were evaluated for the application of inter-metal dielectric (IMD) materials in current devices. Film characteristics were examined as a function of deposition/sputter etch (D/S) ratio, which was controlled by the bias power in HDP-CVD. FTIR spectra show that the positions of Si–O and Si–F peaks are independent of the bias power, but the Si–O shifted to a higher wave number and $Si–F_2$ appeared upon annealing for the films deposited at lower bias power. Stress hysteresis of the FSG films after the first thermal cycle shows a nonequilibrium nature of the microstructure related to impurity content, especially for the film deposited with lower bias power. Thermal desorption of H_2O, F, O_2 and Ar were examined, while most of the desorption behaviour can be related to the physical pore structure and pore quantity.
© 2005 Elsevier B.V. All rights reserved.

Keywords: High-density plasma (HDP) CVD; Bias power; Stress hysteresis; Thermal desorption

1. Introduction

Among all developing low-dielectric materials, fluorine doped silicon oxide (FSG) has been recognized as a promising inter-metal dielectric (IMD) material for its low dielectric constant, which ranges from 3.3 to 3.9 [1–4]. In addition, high gap-filling ability has also been demonstrated for a feature with aspect ratio, AR, of metal line height to metal line separation up to 1.35:1 [5]. In order to successfully integrate this FSG film into the manufacturing processes for sub −0.18 μm technology, high-density plasma chemical vapor deposition (HDP-CVD) is widely employed. The gap filling capability of the HDP CVD film was decided by the ratio of sputter to deposition rate. The HDP-CVD technique consists of both deposition and sputter etch processing, which occur simultaneously at the growing film surface. The sputter etch process is achieved by physical ion bombardment through Ar^+ and O^{2-}, and chemical etching through F^- ions reacted with SiO_2. The sputter etch process was intended for preventing gap seal from deposition process. However, to obtain better gap-filling capability for even smaller sized devices in future, a faster sputter etch rate is required.

Stress in dielectric films is an important issue and becomes more so as the device size continues to decrease. Over the past 20 years, a large number of stress studies about dielectric oxide films prepared by chemical-vapor-deposition (CVD) have been reported [6–10]. In addition, impurity content has also been shown to influence the properties and reliability of the oxide film [11–15]. In this study, detailed characterizations of the FSG films deposited with different bias power and the relationship between impurities and thermal stress are investigated.

2. Experiment

Deposition was performed by a HDP-CVD system operated with gas sources of SiH_4, SiF_4, O_2 and Ar at the

* Corresponding author. Tel.: +886 6 5052000; fax: +886 6 5052057.
E-mail address: ylwang@tsmc.com (Y.L. Wang).

0040-6090/$ - see front matter © 2005 Elsevier B.V. All rights reserved.
doi:10.1016/j.tsf.2005.07.129

Table 1
Sample nomenclature and characteristics of the as-deposited FSG films by HDP-CVD

Samples	Bias power (W)	Deposition rate (nm/s)	D/S ratio	Temperature (°C)
FSG 1	0	8.7	–	338
FSG 2	1000	7.8	9.8	273
FSG 3	2000	6.9	4.8	362
FSG 4	3000	6.1	3.4	438

flow rate of 40, 30, 100 and 45 sccm, respectively. The sample nomenclature is listed in Table 1. The base pressure of the deposition chamber was 5 mTorr, while bias power was varied from 0 to 3000 W. Film thickness was fixed at 740 ± 10 nm by varying deposition time in order to exclude thickness dependence of residual stress. P-type (100) Si wafer of 200 mm in diameter and 725-μm in thickness were used as the substrate on which stress measurements were performed.

The thickness of the FSG films was measured by spectroscopic ellipsometry. Fluorine content in the film was measured using Fourier Transformed Infrared Spectroscopy (FTIR) for active doped fluorine, which was evaluated by the peak ratio of Si–F_x (x = 1, 2) [1] to Si–O, and using X-ray Fluorescence Spectroscopy (XRF) for total fluorine content. FTIR was also used to study the bonding configuration of the films where the spectra were calibrated with a bare silicon substrate. The relative dielectric constant was determined by Mercury Probe at 1 MHz. A commercial curvature measurement tool (Frontier Semiconductor Measurements, FSM900TC) was used to examine film stress in-situ, in which the wafer was heated by six tungsten-halogen lamps in an evacuated chamber at ~10^{-6} Torr. The stress was determined by measuring the change of the substrate curvature induced by the deposited layer. The thermal budget designed in the in-situ stress measurements is from room temperature (25 °C) to 600 °C for three cycles and the heating rate is approximately 10 °C/min. During thermal annealing, thermal desorption spectrometry (TDS) was employed to in-situ monitor the qualitative information of material stability as a function of temperature.

3. Results and discussion

Film deposition rate is dependent on the bias power as given in Table 1, the D/S ratio being varied from 3.4 to 9.8 for the bias power varied from 1000 to 3000 W. Furthermore, the substrate temperature of the FSG2 sample is uncommonly lower than the others, suggesting that the thermal capacity depleted by plasma is higher than input by ion bombardment. Therefore, the FSG film deposited at 1000 W might exhibit different properties to the others.

Fig. 1 shows the variation of fluorine concentration in the FSG films before and after annealing as a function of bias power during deposition. It can be seen from Fig. 1 that the total fluorine concentration of the as-deposited films decreases almost linearly with increasing bias power, from 11.5% to 4.1%. Also, the activated doped fluorine (Si–F_x% x = 1, 2) concentration decreases at a slower rate with increasing bias power from 7.7% to 4%. The difference between these two measurements referred to the free fluorine content in the film. Therefore, this implies that the fluorine was incorporated into the Si–O network more completely when deposited at higher bias power. Moreover, the total fluorine concentration decreases and activated fluorine increases upon annealing for all samples, indicating that the free fluorine becomes chemically reacted into the Si–O network after thermal treatment.

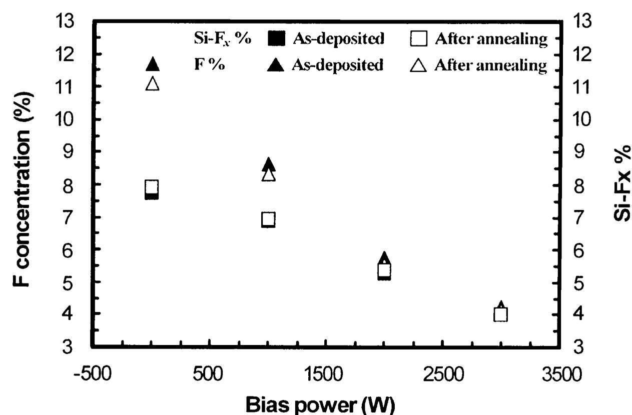

Fig. 1. Total fluorine and Si–F_x concentration variation in the FSG films deposited with various bias powers before and after thermal cycling from 25 °C to 600 °C with the heating rate of 10 °C/min for three times.

As determined by FTIR spectra in Fig. 2, F atoms mainly form Si–F bonds with Si interconnected to the SiO_2 network. The FTIR spectra show the adsorption peaks of the as-deposited FSG (Fig. 2(a)) films at around 1092, 948 and 821 cm^{-1}, corresponding to Si–O stretching mode, Si–F stretching mode, and Si–O bending mode, respectively.

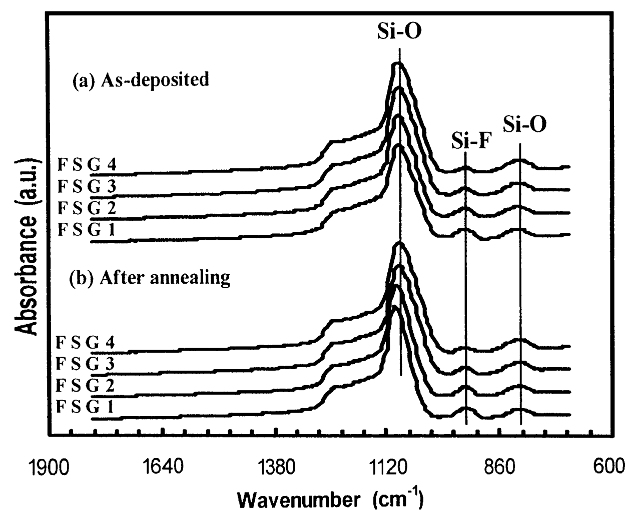

Fig. 2. FTIR spectra showing the bonding configuration of the FSG films before and after the thermal treatment.

However, the Si–O stretching mode of the FSG1 and FSG2 samples shifts to a higher wave number and becomes more intense for all samples upon annealing (Fig. 2(b)). Chou et al. [16] reported that the shift of the Si–O stretching mode to a higher wave number was due to the dissolution of the fluorine atoms as revealed by the upgrade of the Si–F stretching mode located at 948 cm^{-1}. Bhan et al. [1] indicated that with increasing fluorine concentration, the Si–F peak become broadened and intensified, and an additional absorption peak of $Si–F_2$ asymmetrical stretching vibration occurred at 980 cm^{-1}. The change in the Si–O bonding configuration is thought to be related to the presence of the $Si–F_2$ bonds because fluorine has a relatively high electronegativity [17]. In other words, the shift of the Si–O stretching mode to a higher wave number is mainly due to the widening of the Si–O–Si bonding angle [18,19]. In order to identify the $Si–F_2$ peak, the Si–F peaks were magnified in Fig. 3. Apparently, the Si–F stretching mode becomes more intense upon annealing, suggesting more free fluorine incorporated into the SiO_2 network, which agrees with the result from Fig. 1. Furthermore, a small peak is formed at around 980 cm^{-1}, which is the $Si–F_2$ asymmetrical stretching vibration and only from the samples of FSG1 and FSG2.

Stress evolution of the FSG films with bias power is shown in Fig. 4 for the first thermal cycle, where the symbols of the solid and open squares represent data for the heating and cooling cycle, respectively. On the first thermal cycle, all samples exhibit significant film stress hysteresis, and the subsequent heating cycles only yield linear stress hysteresis with smaller magnitude. The nonlinear characteristics in the stress hysteresis result from film stress relaxation and the linear behavior after the first cycle seems to reach thermal equilibrium. The “first-cycling effect” has

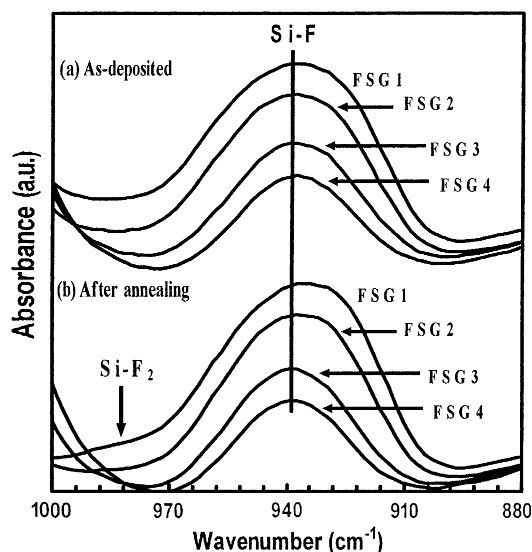

Fig. 3. FTIR spectra of the FSG films exhibiting the effect of the thermal treatment on the Si–F peak intensity, observed at the wave number of 940 cm^{-1}.

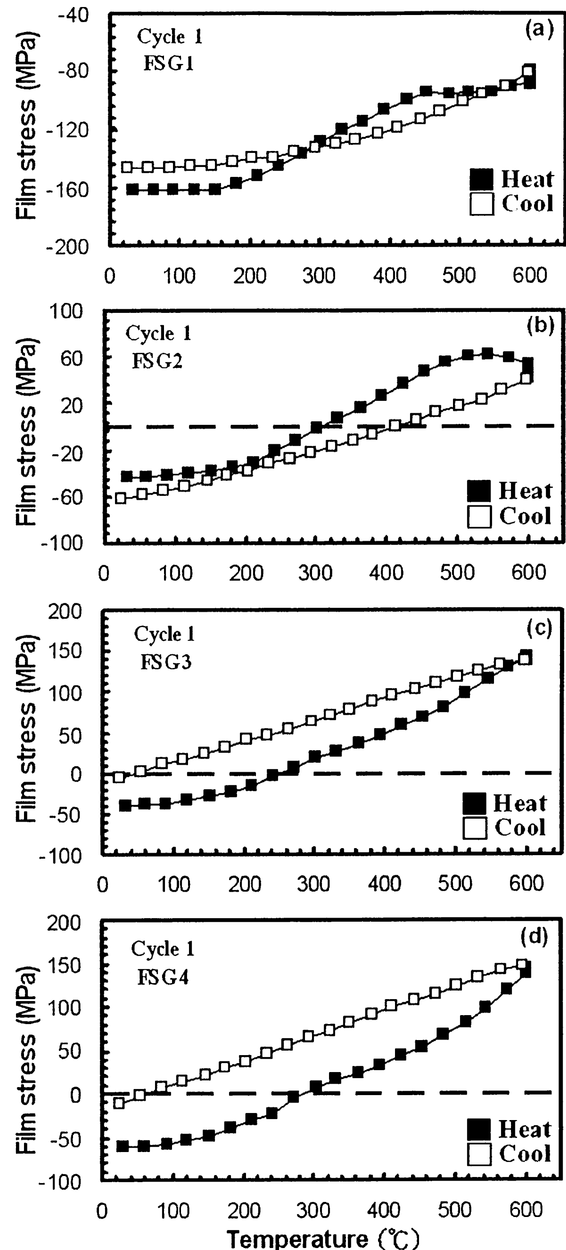

Fig. 4. Film stress as a function of temperature for the HDP-CVD FSG films deposited at the bias of (a) 0 W, (b) 1000 W, (c) 2000 W and (d) 3000 W during the first thermal cycle.

been studied by Thum et al. [6] who ascribed the nonlinear thermal stress to structure or density mismatch between the film and substrate. Therefore, the more nonlinear behavior from FSG1 and FSG2 than the others suggests that microstructure change or even impurity desorption might be involved [6,8,11,12,15] during the first thermal cycle. This compares with the result of Fig. 3 in that additional $Si–F_2$ bond that appeared in the FSG1 and FSG2 samples upon annealing. Apparently, the stress variation of the FSG3 and FSG4 samples behaves similarly during the first thermal cycle indicating that the film quality approaches the same when deposited with higher bias power. The linear region in

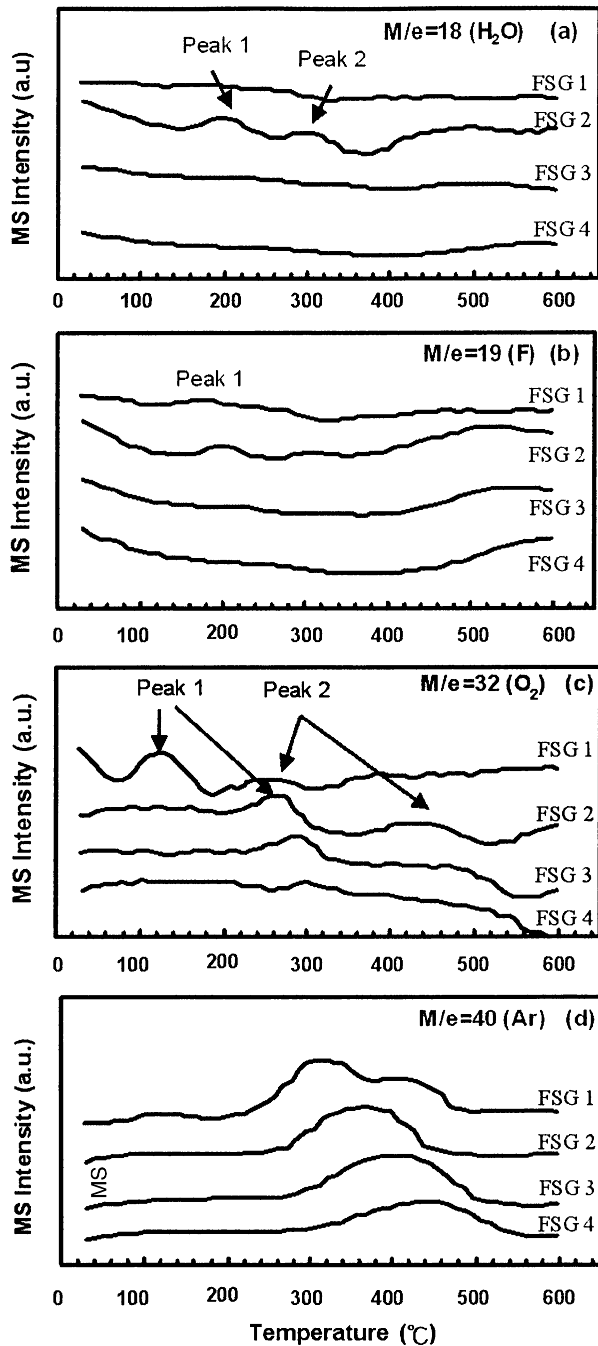

Fig. 5. TDS spectra of the first heating-cycle from the FSG films deposited with different bias power for (a) H_2O (m/e=18), (b) F (m/e=19), (c) O_2 (m/e=32), and (d) Ar (m/e=40).

Fig. 4 is attributed to the thermal expansion mismatch between the film and substrate [6]. Thus, the coefficient of thermal expansion (CTE) of the film, α_f, can be calculated using

$$\frac{d\sigma_f}{dT} = -\frac{E_f}{1-\nu_f}(\alpha_f - \alpha_s) \quad (1)$$

where α_s is the CTE of the Si substrate (α_s=3.0 ppm °C^{-1}). The film CTE is determined from the slope of the linear region, which is proportional to $-(\alpha_f-\alpha_s)$. It can be seen from Fig. 4 that the slope of this region increases slightly with increasing bias power, meaning that the FSG film becomes denser when deposited at higher bias power.

In order to realize the influence of impurity present in the FSG films, thermal desorption spectra (TDS) was in-situ monitored during thermal cycling. Fig. 5 shows TDS spectra from the first heating-half cycle for (a) H_2O (m/e=18), (b) F (m/e=19), (c) O_2 (m/e=32) and (d) Ar (m/e=40). As shown in Fig. 5(a), there are two peaks for water desorption at about 200 °C and 300 °C only from the FSG2 sample, corresponding to the desorption of the absorbed molecular H_2O in the pore structure and hydrogen bonded H_2O to Si–OH, respectively [11]. However, it has been demonstrated that water absorption was dependent on the F concentration in the FSG film and can be stabilized by HDP CVD [12], which might be responsible for the unusual low substrate temperature for the as-deposited FSG2 sample. Fluorine desorption (Fig. 5(b)) occurs as a small peak at about 200 °C only from FSG1 and FSG2 resulting from free fluorine incorporation, which is also related to the desorption of the physically absorbed isotropic water as shown in Fig. 5(a) [13]. Oxygen (m/e=32) desorption spectra in Fig. 5(c) show a small sharp peak at around 130 °C and a broadening desorption peak at around 250 °C from FSG1. Meanwhile, the first peak shifts to higher temperature and the peak area decreases with increasing bias power, indicating that the first peak of O_2 desorption is due to the absorbed molecular O_2 in the pore structure. On the other hand, the broad desorption peak only appears in FSG1 and FSG2, which is ascribed to O_2 from the Si–O bond structure. Ar (m/e=40) can be incorporated in the film during deposition by HDP CVD as shown in Fig. 5(d). Surprisingly, the Ar desorption peak is located at around 320 °C, 370 °C, 400 °C and 440 °C for FSG1, FSG2, FSG3 and FSG4, respectively. The Ar desorption must be related to the pore structure of the FSG films, and the peak area represents the pore quantity. The

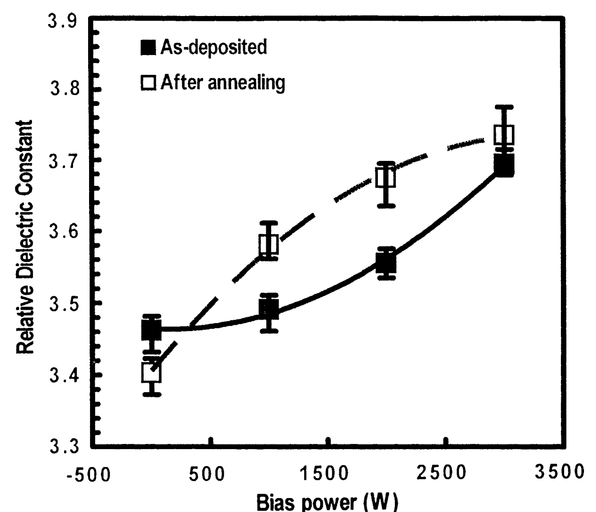

Fig. 6. Relative dielectric constant of the FSG films deposited with various bias powers, where the symbols of solid and open squares are as-deposited and annealed films, respectively.

smaller peak area with the less pore quantity is consistent with the denser film deposited at higher bias power. Fig. 5 demonstrates that the bias power strongly affects the FSG film quality.

The relative dielectric constant of the FSG films before and after annealing with various bias powers is shown in Fig. 6. Apparently, the dielectric constant increases with increasing bias power from 3.46 to 3.69, and also increases upon annealing except FSG1. The decreased dielectric constant of FSG1, which was deposited without bias power, means that the $Si-F_2$ bond formation and most of impurities desorped. Therefore, these results show that bias power affects film properties significantly.

4. Conclusions

In this study, the characteristics of the as-deposited FSG films by HDP CVD were investigated as a function of bias power. Substrate temperature increases due to ion bombardment when deposited with higher bias power. Fluorine concentration was also found to be dependent on the bias power. For the as-deposited FSG films, both total fluorine and activated Si–F concentration increase with increasing bias power leading to free fluorine decreasing. However, FTIR spectra show that Si–O and Si–F peak positions are independent of the bias power. After the thermal treatment, the Si–O peak shifts to a higher wave number and $Si-F_2$ appears at around 980 cm^{-1} when deposited with lower bias power, suggesting more fluorine incorporation upon annealing. Stress hysteresis examination exhibits nonequilibrium behavior for the first thermal cycle, especially for the film deposited with lower bias power, which resulted from the microstructure change and the evolution of impurities in the FSG films. From TDS spectra, the films deposited at lower bias power desorb H_2O, O_2, F and Ar of different amount at different temperature depending on the actual bias power used, while those deposited at higher bias power only desorb O_2 and Ar. Most of the impurity desorption can be related to the physical pore structure and pore quantity. In conclusion, deposition bias power is a key factor in obtaining high quality FSG films.

Acknowledgements

The authors gratefully acknowledge the help from Taiwan Semiconductor Manufacture Company, Taiwan in providing the samples and analytical equipments.

References

[1] M.K. Bhan, J. Huang, D. Cheung, Thin Solid Films 308–309 (1997) 507.
[2] M.J. Shapiro, S.V. Nguyen, T. Matsuda, D. Dobuzinsky, Thin Solid Films 270 (1995) 503.
[3] G. Passemard, P. Fugier, P. Noel, F. Pires, Microelectron. Eng. 33 (1997) 335.
[4] S. Mizuno, A. Verma, H. Tran, Thin Solid Films 283 (1996) 30.
[5] J.K. Lan, Y.L. Wang, Y.L. Wu, Thin Solid Films 377–378 (2000) 776.
[6] J. Thurn, R.F. Cook, M. Kamarajugadda, J. Appl. Phys. 91 (2002) 1988.
[7] J. Thurn, R.F. Cook, J. Appl. Phys. 95 (2004) 967.
[8] B. Bhushan, S.P. Murarka, J. Gerlach, J. Vac. Sci. Technol., B 8 (1990) 1068.
[9] S.P. Kim, S.K. Choi, Thin Solid Films 379 (2000) 259.
[10] M.S. Haque, H.A. Nasseem, W.D. Brown, J. Appl. Phys. 82 (1997) 2922.
[11] M. Yoshimaru, S. Koizumi, K. Shimokawa, J. Vac. Sci. Technol., A, Vac. Surf. Films 15 (1997) 2915.
[12] H. Miyajima, R. Katsumata, Y. Nakasaki, Jpn. J. Appl. Phys. 35 (1996) 6217.
[13] T. Tamura, J. Sakai, M. Satoh, Jpn. J. Appl. Phys. 38 (1999) 6571.
[14] N. Hirashita, S. Tokitoh, H. Uchida, Jpn. J. Appl. Phys. 32 (1993) 1787.
[15] G. Vereecke, E. Kondoh, P. Richardson, IEEE Trans. Semicond. Manuf. 13 (2000) 315.
[16] J.S. Chou, S.C. Lee, J. Appl. Phys. 77 (1995) 1805.
[17] S. Lee, J.W. Park, J. Appl. Phys. 80 (1996) 5260.
[18] G. Lucovsky, J.T. Fitch, D.V. Tsu, S.S. Kim, J. Vac. Sci. Technol., A, Vac. Surf. Films 7 (1988) 1136.
[19] J.T. Fitch, G. Lucovsky, E. Kobeda, E.A. Irene, J. Vac. Sci. Technol., B 7 (1989) 153.